

Investigation on arrangement and fusion behaviors of gold nanoparticles at the air/water interface

Lihua Pei¹, Koichi Mori², Motonari Adachi^{*}

Institute of Advanced Energy, Kyoto University, Uji, Kyoto 611-0011, Japan

Received 23 August 2005; received in revised form 30 December 2005; accepted 13 February 2006

Available online 6 March 2006

Abstract

The arrangement and fusion behavior of alkanethiol-stabilized gold nanoparticles were investigated at the air/water interface by the Langmuir–Blodgett (LB) method using two different organic solvent, toluene or hexane. The results showed that the organic solvent greatly affected the arrangement and fusion behavior of the gold particles. In the case of toluene solvent, alkyl chains of alkanethiol combined to gold particles spread out, and the diameter of the gold particles became almost equal with each other, resulting in the spontaneous ordered arrangement in closed packed array by self-organization. The fusion of particles was clearly confirmed from the lattice image of the fused particles observed by high-resolution transmission electron microscopy (TEM). The difference in the arrangement and fusion of the nanoparticles caused by the organic solvent was a result of the different affinity of the organic solvent with the alkyl chain of alkanethiol, which can be predicted using the solubility parameter.

© 2006 Elsevier B.V. All rights reserved.

Keywords: Gold nanoparticle; Arrangement; Fusion; Solvent effect; LB method

1. Introduction

Nanostructures has attracted steadily growing interest due to fascinating properties and intriguing applications [1]. Much of this interest is powered by the growing expertise in fabrication methods that allow more ways of realizing nanostructures with well-controlled composition, size, and shape. The fundamental study of phenomena that occur in nanostructured materials has already evolved into a new field of research, i.e., nanoscience. The role of nanoscience is indispensable for development of a broad range of emerging and exciting applications such as more powerful computer chips and higher-density information storage through nanostructural control.

The interaction of light with free electrons in a gold nanostructure can give rise to collective excitations commonly known as surface plasmons. Plasmons provide a powerful means of confining light to metal/dielectric interface, which in turn can generate intense local electromagnetic fields and significantly amplify the signal desired from analytical techniques such as Raman scattering. With plasmons, photonic signals can be manipulated on the nanoscale, enabling integration with electronics. However, to benefit from their interesting plasmonic properties, metal structure of controlled shape and arrangement must be fabricated on the nanoscale [2]. When the sample contains an ensemble of nanoparticles supported on a substrate, the extinction spectrum of localized surface plasmon resonance depends on inter-particle spacing and substrate dielectric constant, as well as on the diameter of nanoparticles, out-of-plane height, and shape [3,4]. These parameters should be precisely controlled in nano-scale.

Highly ordered monolayer of nanosized surfactant stabilized metal particles was fabricated using Langmuir–Blodgett (LB) method [5–8]. Recently, two-dimensional network of gold nanowires or cross-linked nanoparticle networks were formed by self-assembly of gold nanoparticles on water surface using LB technique [9–12]. Thus, LB technique is quite suitable for highly ordered arrangement of gold nanoparticles and forma-

^{*} Corresponding author. Present address: International Innovation Center, Kyoto University c/o Isoda Laboratory The Institute for Chemical Research, Kyoto University, Uji, Kyoto 611-0011, Japan. Tel.: +81 774 38 4538; fax: +81 774 38 3055.

E-mail address: adachi@iae.kyoto-u.ac.jp (M. Adachi).

¹ Present address: Information and Electronics Division of Mitsubishi Chemical Corporation, Japan.

² Present address: Solution and Technology Department of Air Water Inc., Japan.

tion of gold nanowires. As for fusion of gold nanoparticles, some researchers reported that fusion occurred spontaneously [13–15] and others assert that the cross-linked process was effected at high surface pressures, and nanocrystals seem to coalesce only when sufficient capping ligand has been removed [10–12]. When the particles approach within 5 Å, strong metallic bonding could help to drive nanocrystal adhesion and subsequent coalescence [12]. In our previous work, network structure of gold nanowires also has been formed by fusion of nanoparticles by a hit-to-stick-to-fusion model, i.e., gold nanoparticles adhere by the attraction force and stick together by jump-in when the two particles approach within 10 Å, followed by fusion into nanowires [16]. Effect of solvent was also investigated as an important factor for fabrication of high-quality of monolayer of alkanethiol-encapsulated gold nanoparticles. The observed great effect was unfortunately explained mainly based on the evaporation rate of solvents [8]. It is well known, however, that the preferential solvation and penetration of solvents into the hydrophobic surfactant chains are the main effect of solvent to determine the shape of the molecular assemblies composed of surfactants and water [17–20]. In reverse micellar system, penetration of solvent molecules into the monolayer of surfactant tails causes the increase in the effective volume of the hydrocarbon part of the monolayer, resulting in the decrease in the diameter of reverse micelles. The diameter of the reverse micelles is strongly influenced by the solvent species.

From the situation mentioned above, fundamental phenomena observed in the processes of fabricating metal structure of controlled shape and arrangement have not been understood sufficiently.

In this article, we present fundamental research on the effect of solvent for arrangement of alkanethiol-capsulated gold nanoparticles and nanowire formation through fusion of gold nanoparticles under high surface pressure using Langmuir–Blodgett method.

2. Experimental

2.1. Materials

Sodium tetrachloroaurate(III) ($\text{NaAuCl}_4 \cdot 2\text{H}_2\text{O}$), hexane, toluene and ethanol (99.5%) were purchased from Nacalai Tesque Inc. Didodecyldimethylammonium bromide (DDAB) was obtained from Tokyo Chemical Industry Co. Sodium borohydride (95%) was purchased from Wako Chemicals. Alkanethiol used were 1-dodecanethiol (Nacalai Tesque).

2.2. Synthesis of gold nanoparticles

The colloid gold particles used in this work were synthesized by reducing sodium tetrachloroaurate (NaAuCl_4) with sodium borohydride (NaBH_4) in a reverse micellar system. Typically, the synthesis was carried out by the following procedure: first, DDAB was dissolved in 100 mL cyclohexane (0.2 M) at 40 °C, and 2.5 mL of 0.1 M NaAuCl_4 aqueous solution was added for complete mixing. The water content in the reverse micellar phase was measured by the Karl–Fisher method (AQ-6, HIRANUMA)

[21,22]. After the equilibrium, the water-to-DDAB mole ratio, W_0 was determined to be 5.8. Then a controlled amount of ice-freshly prepared NaBH_4 solution (3.69 M) was added in this mixed solution. Upon addition of NaBH_4 , the reaction solution gradually turned yellow, colorless and deep pink–purple, indicating the formation of gold nanoparticles. Subsequently, excess alkanethiol was added to protect the gold nanoparticles. This mixed solution was kept for at least one night. Finally, the same volume of ethanol was added to the resulting solution to precipitate the gold particles, followed by centrifugation at 6000 rpm for 10 min. The supernatant was removed and the precipitate was dispersed in ethanol and centrifuged again. This step was repeated for five times to completely remove the surfactants.

2.3. Preparation of gold suspension in organic solvents

After the above centrifugation, the precipitates of alkanethiol-capped gold particles were dispersed in organic solvents using an ultrasonic processor. In this work, two kinds of organic solvents were used, toluene and hexane, which are typical of aromatic and aliphatic structure, respectively. The concentration of gold particles in the suspension was determined using an inductively coupled argon plasma emission spectrophotometer (ICAP-500, Nippon Jarrell Ash Co.) device. In this work, we prepared alkanethiol-capped gold particle suspensions with concentration of about 0.6 mg/mL. The well-dispersed suspension was stable and can be stored at room temperature for at least one month.

2.4. Compression of gold nanoparticles on the LB trough

The LB instrument used in this work was a FSD-220 (USI SYSTEM CO., Ltd.) instrument. The sub-phase (water of 18.2 M Ω) temperature was controlled at 20 °C for all the experiments. The gold suspension solution was spread carefully onto the surface of pure water at intervals of 15 s. After evaporation of solvent for about 30 min, the particles were compressed by moving the barriers at a constant speed of 0.5 mm/s. The surface pressure–area (π – A) isotherm was recorded throughout the LB compression. At desired surface pressure, the gold particles were transferred to the carbon-coated copper grids by horizontal lifting for transmission electron microscopy (TEM) observation. TEM and high-resolution transmission electron microscopy (HRTEM) images of the sample were measured using JEOL JEM 200CX equipment at an accelerating voltage of 200 kV.

3. Results and discussion

3.1. Characterization of gold nanoparticles

In the present work, nanoparticles were synthesized in a reverse micellar system and capped with alkanethiol, then suspended in organic solvents, such as hexane and toluene, respectively, to obtain stable gold suspensions. The observed mean core diameter of the particles was 4.8 nm, with a standard deviation of 0.6 nm. These particles are crystalline and polyhedron shaped,

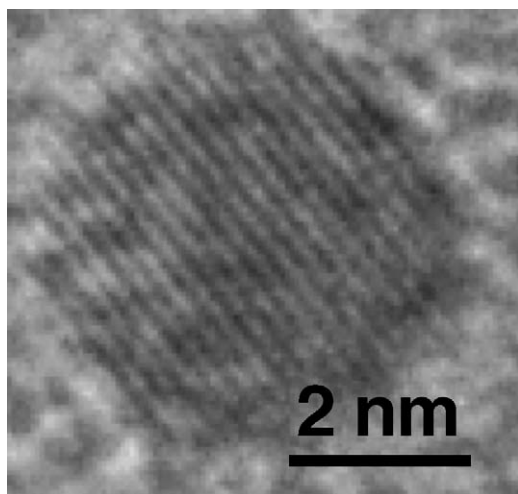


Fig. 1. TEM image of a 4.8-nm-diameter colloidal gold particle. The lattice fringe is about 0.24 nm, which is in agreement with the spacing between Au (1 1 1) planes.

such as icosahedrons and decahedrons. TEM observation shows that the shape of the gold particles is mostly spherical-like. Fig. 1 is a HRTEM image of gold particle with diameter of about 4.8 nm. The lattice fringe is about 0.24 nm, which is in agreement with the spacing between Au (1 1 1) planes.

3.2. Pressure–area (π -A) isotherms

The behavior of thiol-capped gold particles at the air–water interface was characterized through pressure–area (π -A) isotherms. Fig. 2a shows a π -A isotherm for the gold suspension dispersed in hexane. Upon compression, gold particles form a

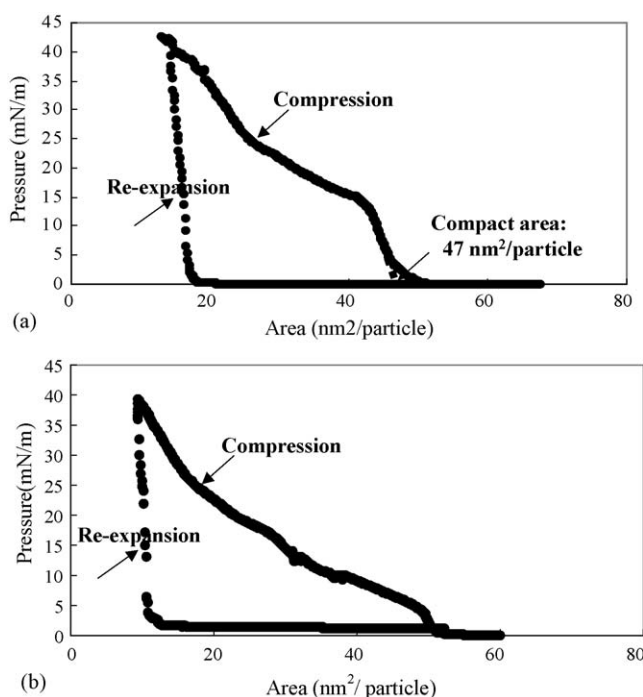


Fig. 2. Compression isotherm of dodecanethiol-capped gold particles dispersed in hexane (a) and toluene (b), respectively.

stable monolayer at the air–water interface. It can be seen that the surface pressure increased abruptly from 0 mN/m at the area about 50 nm²/particle to 15 mN/m at the area of 42 nm²/particle. The pressure increased mildly from 15 mN/m at 42 nm²/particle to 25 mN/m at 25 nm²/particle. Then, the pressure increased steeply again to 43 mN/m at 14 nm²/particle. At surface area of 14 nm²/particle, the barrier trough was re-expanded. The re-expansion curve did not go back along the compression curve with a large hysteresis, indicating that the compression and relaxation processes were not reversible when the sample was compressed up to 43 mN/m, and the monolayer of gold nanoparticles did not collapse but kept its morphology well. We confirmed that the (π -A) isotherm showed reversible behavior when the surface pressure was less than 25 mN/m.

By extrapolating the straight part of the π -A isotherms from higher pressures (15 mN/m) to zero, the compact area could be estimated to be 47 nm² per particle assuming a dense packing [6]. This value is in good agreement with the calculated value of the hexagonal closed packed area 48 nm² per particle for particles with diameter of 4.8 nm.

Fig. 2b shows a π -A isotherm for the gold suspension in toluene solvent. The surface pressure increased abruptly from 0 mN/m at area about 51 nm²/particle to 5 mN/m at the area 48 nm²/particle. Then, the pressure increased mildly from 5 mN/m at 48 nm²/particle to 25 mN/m at 17.5 nm²/particle. The pressure, then, increased steeply to 40 mN/m at 9.5 nm²/particle. At surface area 9.5 nm²/particle, the barrier trough was re-expanded. The re-expansion curve also showed hysteresis, indicating that relaxation process could not collapse the structure formed at high surface pressure 40 mN/m, and rather the formed structure was kept until the surface pressure was reached near 0 mN/m. The compact area in the toluene system can be obtained by extrapolating the straight part of the π -A curve from higher pressure (5 mN/m) to 0 mN/m to be 50 nm²/particle, which is also very close to the calculated value of the hexagonal closed packed area 48 nm². These agreements observed in both systems indicate that the surface pressure started to increase in nearly closed packed state of nanoparticles.

3.3. Transmission electron microscopy observations

Fig. 3 shows the TEM images of dodecanethiol-capped gold particles at different surface pressures transferred from hexane solvent. When the surface pressure was 0 mN/m, gold nanoparticles were randomly spread at the water surface with many voids, as shown in Fig. 3a. When the barrier was moved to 13 mN/m, most of the voids disappeared and a hexagonal closed-packed monolayer was formed as shown in Fig. 3b. However, when particles were further compressed to a high surface pressure, 36 mN/m, particles were connected to a network structure mixed with some isolated particles (Fig. 3c). In the case of toluene solvent, gold nanoparticles formed a closed-packed monolayer before compression (Fig. 4a). This result implied that the ordered arrangement of gold nanoparticles were not caused by compression, but caused by a self-organization process induced by the evaporation of solvent in the spreading suspension before LB compression when particle size was uniform as shown later

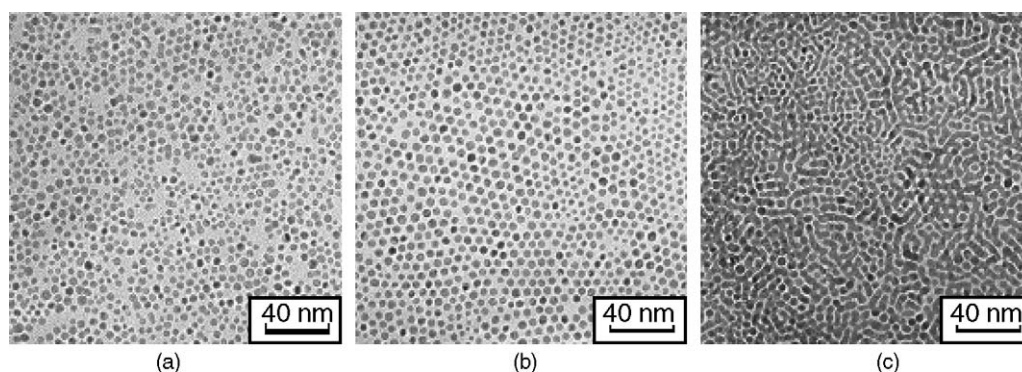


Fig. 3. TEM images of dodecanethiol-capped gold particles transferred at the surface pressure of (a) 0 mN/m, (b) 13 mN/m, and (c) 36 mN/m, respectively. The particles before compression was dispersed in hexane solvent.

[8]. It should be mentioned that when the barrier was moved to 36 mN/m, most of the particles were fused to nanowires (Fig. 4c).

Fig. 5 shows the HRTEM images of gold particles dispersed in toluene and hexane, respectively, under high-pressure range (36 mN/m). As shown in Fig. 5a for the case of toluene solvent, several gold nanoparticles with diameter of about 5 nm fused with each other and made straight nanowires of length with several tens nm. Lattice images of Au (1 1 1) crystalline phase were clearly observed, and the crystalline directions aligned perfectly over several particles, showing strongly occurrence of fusion of gold nanoparticles. As for the case of hexane solvent (Fig. 5b), several gold nanoparticles were also fused, but the shape of nanowires was not straight, but worm-like. Lattice images of Au (1 1 1) crystalline phase also were observed, indicating occurrence of fusion of nanoparticles with each other, but the crystalline directions of particles did not align with each other.

Let us consider the reason of fusion between nanoparticles. In the present work, fusion of nanoparticles was observed under high surface pressure (36 mN/m). When the surface pressure is transformed to usual pressure assuming that the thickness of the contact between nanoparticles is the half of the diameter of the particles (2.4 nm), the pressure could be calculated as:

$$\frac{36 \times 10^{-3}}{2.4 \times 10^{-9}} = 15 \times 10^6 \text{ Pa} = 150 \text{ atm}$$

Since the actual contact area is expected to be less than the above value, the pressure is inferred to be much larger. We consider that high-pressure compression induce the removal of capping alkanethiol molecules from the surface of gold particles, resulting in the fusion of gold nanoparticles into nanowires. Korgel and Fitzmaurice [12] reported similar reasoning, i.e., nanocrystals seem to coalesce only when sufficient capping ligand has been removed, and the particles approach within 5 Å as described in Section 1.

From the above experimental results, great effects of solvent are observed in the fabrication process of nanostructures of controlled arrangement and shape.

- (1) In the system with toluene solvent, highly ordered array of nanoparticles was obtained spontaneously under no surface pressure, 0 mN/m. In comparison with the toluene system, random arrangement of nanoparticles was observed at 0 mN/m in the system with hexane solvent.
- (2) Straight nanowires with single crystal were obtained at high surface pressure (36 mN/m) in the system with toluene solvent. Crystalline directions of nanoparticles constituting the nanowire were completely aligned. In comparison with the toluene system, nanowires of worm-like shape with polycrystalline structure were obtained at high surface pressure (36 mN/m) in the system with hexane solvent.

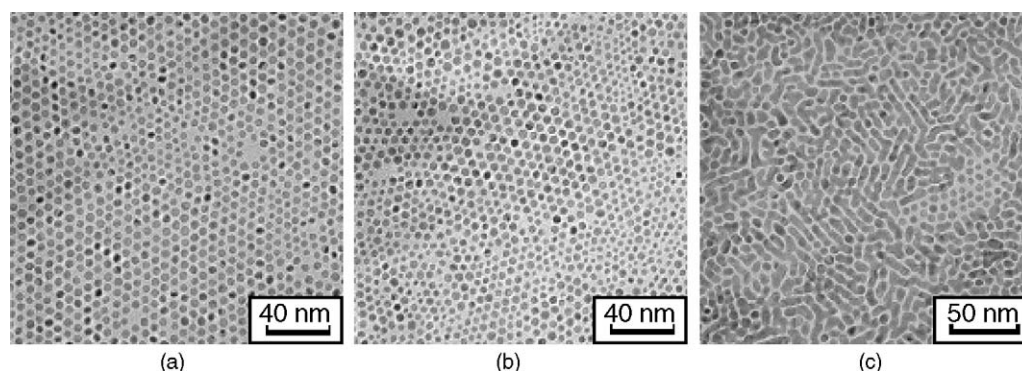
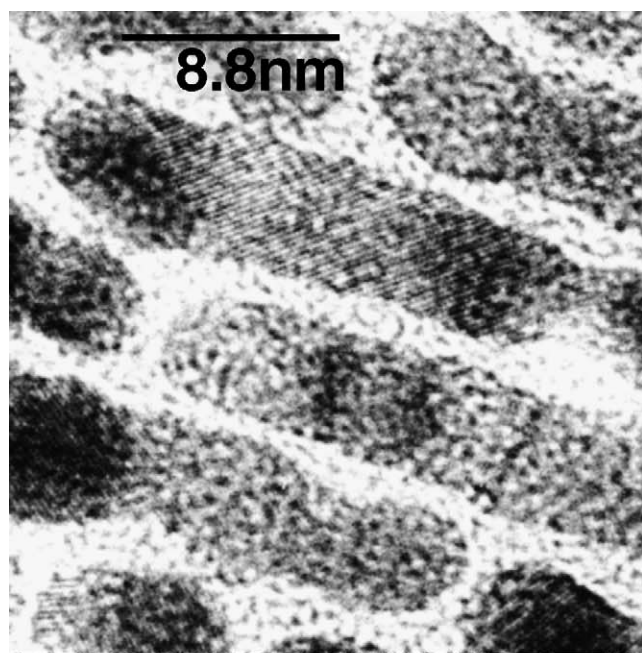
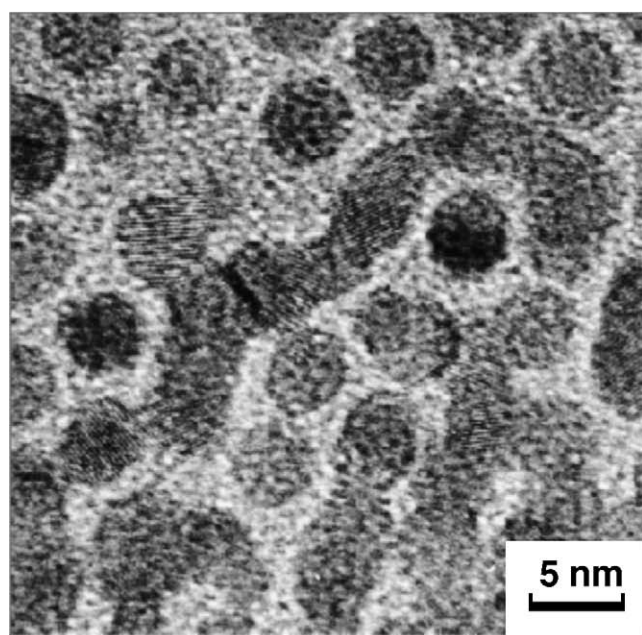


Fig. 4. TEM images of dodecanethiol-capped gold particles transferred at the surface pressure of (a) 0 mN/m, (b) 10 mN/m, and (c) 36 mN/m, respectively. The particles before compression was dispersed in toluene solvent.



(a)



(b)

Fig. 5. HRTEM images of dodecanethiol-capped gold particles transferred at the surface pressure of 36 mN/m. The particles used before compression was dispersed in (a) toluene and (b) hexane solvent, respectively.

3.4. Insight into the solvent effect

As described in Section 1, the preferential solvation and penetration of various solvents into reverse micellar tails composed of hydrocarbon chains has been widely investigated by measuring the diameter of the spherical reverse micelles [20] or using UV–vis absorption probes [18]. Reverse micellar system is one of the most suitable system to investigate the preferential solvation and penetration of the solvent into the monolayer of surfactant tails composed of hydrocarbon chains, because the penetration of solvent into the monolayer causes increase in the hydrocarbon part, i.e., change in the value of packing parameter, which controls the size and shape of the molecular assemblies composed of surfactant molecules [26]. The diameter of the water pool of spherical reverse micelles is strongly influenced by the solvent species, and the preferential solvation and penetration of solvents is reported to be in the order benzene > cyclohexane > *n*-pentane > *n*-hexane > *n*-heptane [20]. From the results obtained in reverse micellar systems, aromatic solvents have properties of stronger preferential solvation and penetration into the monolayer composed of hydrocarbon chains than that of aliphatic solvents.

On the other hand, the dispersion properties of dodecanethiol-capped gold nanoparticles was investigated in various organic solvents by Haung et al. [25]. The system is much closer to our experimental system. They found that the strong affinity of solvents to the capping molecules, which are dodecanethiol, shows better dispersion of nanoparticles. Also they proposed that the interaction between the capping molecules and the solvent can be estimated by the solubility parameter (SP). In general, affinity of the solvent to the capping molecule is high when the SP of the solvent is closer to that of the capping molecule.

In this work we used toluene as an aromatic solvent and hexane as an aliphatic solvent. As shown in Table 1, SP-value of toluene is much closer to dodecanethiol than that of hexane, indicating that affinity of toluene to the dodecanethiol is much higher than that of hexane. This supports the insight obtained from the investigations in the reverse micellar systems.

According to the above insight, we can explain the experimental results obtained in this work as follows. It is well known that a key factor for highly ordered two-dimensional array of nanoparticles is monodispersion in size of the particles [12,23,24]. In the case of toluene solvent, toluene penetrates strongly to the monolayer of dodecanethiol, and alkyl chains of dodecanethiol spread out from the gold particle as shown in Fig. 6. Thus, the diameter of the gold particles becomes almost equal with each other, resulting in the spontaneous ordered arrangement in closed packed array by self-organization. On the other hand, penetration of hexane to the monolayer is much

Table 1
Solubility parameter of capping thiol and solvents

	Dodecanethiol	Chloroform	Toluene	Cyclohexane	Hexane	Water
Solubility parameter	17.6	18.7	18.3	16.8	14.9	48
Difference to dodecanethiol	0	1.1	0.7	−0.8	−2.7	30.4

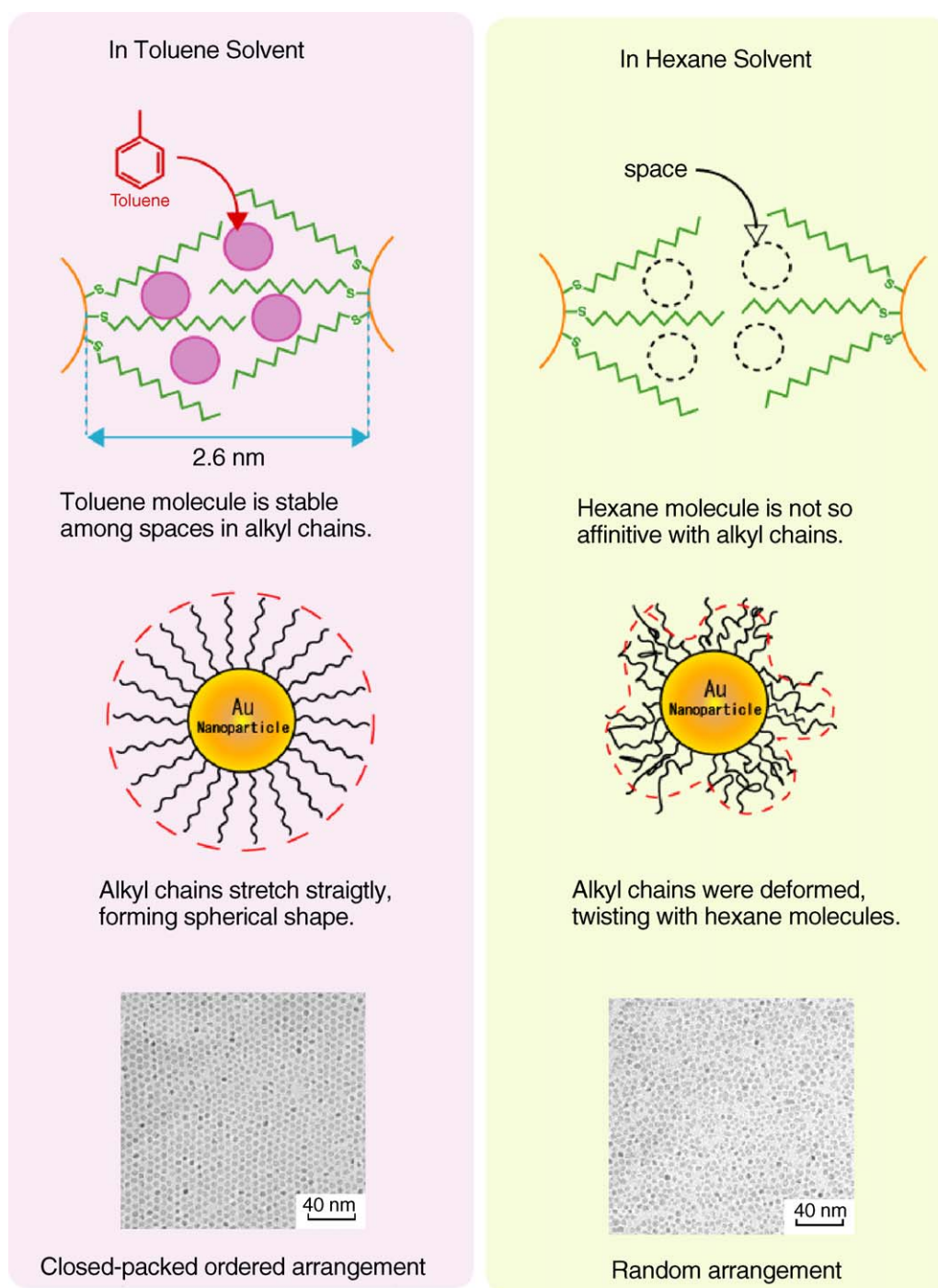


Fig. 6. Schematic illustration of affinity of organic solvent with alkyl chain of dodecanethiol.

weaker, and the hydrocarbon chains interact directly with each other, resulting in deformation and twisting shown in Fig. 6. Thus, nanoparticles take random arrangement under no surface pressure 0 mN/m.

Next, let us consider the variation in the conformational state of nanoparticles under various surface pressures. With compression of the gold nanoparticles, an abrupt increase in surface pressure was observed in both systems. The compact area was estimated to be 47 nm²/particle for the hexane system and to be 50 nm²/particle for the toluene system. These values are very

close to the calculated value for the hexagonal closed packed area 48 nm²/particle, indicating that the surface pressure starts to increase approximately in the hexagonal closed packed state.

When surface pressure increased to 25 mN/m, the occupied area per particle in toluene solvent system 17.5 nm²/particle became smaller than that of hexane solvent system 25 nm²/particle. With further increase in the surface pressure, toluene solvent system took 9.5 nm²/particle at 40 mN/m, and hexane solvent system took 14 nm²/particle at 43 mN/m. The above observations can be interpreted as follows. In toluene

solvent system, nanoparticles basically align in highly ordered closed packed array spontaneously by self-organization, resulting in formation of straight single crystalline nanowires at high surface pressure. Thus, the fraction of fused nanoparticles is high, i.e., the fraction of remaining isolated particles is low. In comparison with the toluene solvent system, nanoparticles in hexane solvent system take random arrangement basically, resulting in the formation of worm-like nanowires at high surface pressure. Thus, the fraction of fused nanoparticles is low, i.e., the occupied area per particle becomes large in the high surface pressure range.

Thus, our experimental results obtained under various surface pressure can be explained according to the insight mentioned above.

Consequently, it is very important to make highly ordered array by self-organization at no surface pressure in order to achieve the fabrication of metal nanostructures of controlled arrangement and shape. To realize this, fabrication of nanoparticles with monodispersion in size and selection of solvent with high affinity to the capping molecule are essential.

4. Conclusion

The solvent effect on the arrangement and fusion behavior of alkanethiol-stabilized gold nanoparticles was investigated at the air/water interface using the Langmuir–Blodgett method in the two different system using toluene or hexane. π - A isotherms, TEM and high resolution TEM images showed that the organic solvent greatly affected the arrangement and fusion behavior of the gold particles.

In the system with toluene solvent, highly ordered array of nanoparticles was obtained spontaneously under no surface pressure, 0 mN/m. In comparison with the toluene system, random arrangement of nanoparticles was observed at 0 mN/m in the system with hexane solvent.

Straight nanowires with single crystal were obtained at high surface pressure (36 mN/m) in the system with toluene solvent. Crystalline directions of nanoparticles constituting the nanowire were completely aligned. In comparison with the toluene system, nanowires of worm-like shape with polycrystalline structure were obtained at high surface pressure (36 mN/m) in the system with hexane solvent.

These effects were interpreted through the difference in the affinity between the solvent and alkanethiol molecule, which can be predicted using the solubility parameter.

Acknowledgment

The authors gratefully acknowledge Professor S. Isoda (Institute for Chemical Research, Kyoto University) for assistance with the TEM observation.

References

- [1] M. Di Ventra, S. Evoy, J.R. Heflin Jr. (Eds.), *Introduction to Nanoscale Science and Technology*, Kluwer Academic Publications, Boston, 2004.
- [2] Y. Xia, N.J. Halas, *MRS Bull.* 30 (2005) 338–343.
- [3] C.L. Haynes, R.P. Van Duyne, *J. Phys. Chem. B* 105 (2001) 5599–5611.
- [4] A.J. Haes, C.L. Hynes, A.D. McFarland, G.C. Schatz, R.P. Van Duyne, S. Zou, *MRS Bull.* 30 (2005) 368–375.
- [5] F.C. Meldrum, N.A. Kotov, J.H. Fendler, *Mater. Sci. Eng., C* 3 (1995) 149.
- [6] L.F. Chi, S. Rakers, M. Hartig, H. Fuchs, G. Schmid, *Thin solid Films* 327 (1998) 520.
- [7] J.P. Bourgoin, C. kergueris, E. Lefevre, S. palacin, *Thin Solid Films* 327 (1998) 515.
- [8] S. Huang, G. Tsutsui, H. Sakaue, S. Shingubara, T. Takahagi, *J. Vac. Sci. Technol. B* 19 (2001) 115;
S. Huang, G. Tsutsui, H. Sakaue, S. Shingubara, T. Takahagi, *J. Vac. Sci. Technol. B* 19 (2001) 2045.
- [9] S.W. Chung, G. Markovich, J.R. Heath, *J. Phys. Chem. B* 102 (35) (1998) 6685.
- [10] S. Chen, *Adv. Mater.* 12 (2000) 186;
S. Chen, *Langmuir* 17 (2001) 2878.
- [11] L. nan, M. Gleiche, L. Chi, H. Fuchs, *Nano Lett.* 2 (7) (2002) 709.
- [12] B.A. Korgel, D. Fitzmaurice, *Adv. Mater.* 10 (9) (1998) 661–665.
- [13] C.J. Kiely, J. Fink, M. Brust, D. Bethell, D.J. Schiffrin, *Nature* 396 (1998) 444.
- [14] T. Yonezawa, S. Onoue, N. Kimizuka, *Chem. Lett.* 12 (2002) 1172.
- [15] T. Yonezawa, S. Onoue, N. Kimizuka, *Adv. Mater.* 13 (2001) 140–142.
- [16] L. Pei, K. Mori, M. Adachi, *Langmuir* 20 (2004) 7837.
- [17] C.L. Kitchens, M.C. McLeod, C.B. Roberts, *J. Phys. Chem. B* 107 (2003) 11331–11338.
- [18] C.B. Roberts, J.B. Thompson, *J. Phys. Chem. B* 102 (1998) 9074–9080.
- [19] A. Goto, H. Yoshioka, H. Kishimoto, T. Fujita, *Langmuir* 8 (1992) 441–445.
- [20] A. Shioi, M. Harada, M. Tanabe, *J. Phys. Chem.* 97 (1993) 8281–8288.
- [21] A. Aelion, A. Loebel, F. Eirich, *J. Am. Chem. Soc.* 72 (1950) 5705.
- [22] M. Harada, S. Itakura, A. Shioi, M. Adachi, *Langmuir* 17 (2001) 4189.
- [23] C. Petit, A. Taleb, M.-P. Pileni, *Adv. Mater.* 10 (1998) 259–261.
- [24] A. Courty, C. Ferman, M.-P. Pileni, *Adv. Mater.* 13 (2001) 254–258.
- [25] S. Huang, K. Minami, H. Sakaue, S. Shingubara, T. Takahagi, *J. Appl. Phys.* 92 (12) (2002) 7486–7490.
- [26] J.N. Israelachvili, *Intermolecular and Surface Forces*, second ed., Academic Press, London, 1992.